Microfluidic Patterning of Miniaturized DNA Arrays on Plastic Substrates

Matthias Geissler,* Emmanuel Roy, Gerardo A. Diaz-Quijada, Jean-Christophe Galas, and Teodor Veres

Industrial Materials Institute, National Research Council of Canada, Boucherville, Québec J4B 6Y4, Canada

ABSTRACT This paper describes the patterning of DNA arrays on plastic surfaces using an elastomeric, two-dimensional microcapillary system (μCS). Fluidic structures were realized through hot-embossing lithography using Versaflex CL30. Like elastomers based on poly(dimethylsiloxane), this thermoplastic block copolymer is able to seal a surface in a reversible manner, making it possible to confine DNA probes with a level of control that is unparalleled using standard microspotting techniques. We focus on μCSs that support arrays comprising up to 2 × 48 spots, each being 45 μm in diameter. Substrates were fabricated from two hard thermoplastic materials, poly(methylmethacrylate) and a polycyclic olefin (e.g., Zeonor 1060R), which were both activated with 1-ethyl-3-[3-(dimethylamino)propyl]carbodiimide hydrochloride and *N*-hydroxysuccinimide to mediate covalent attachment of DNA molecules. The approach was exemplified by using 0.25−32 μM solutions of amino-modified oligonucleotides labeled with either Cy3 or Cy5 fluorescent dye in phosphate-buffered saline, allowing for a direct and sensitive characterization of the printed arrays. Solutions were incubated for durations of 1 to >48 h at 22, 30, and 40 °C to probe the conditions for obtaining uniform spots of high fluorescence intensity. The length (l) and depth (d) of microfluidic supply channels were both important with respect to depletion as well as evaporation of the solvent. While selective activation of the substrate proved helpful to limit unproductive loss of oligonucleotides along trajectories, incubation of solution in a humid environment was necessary to prevent uncontrolled drying of the liquid, keeping the immobilization process intact over extended periods of time. When combined, these strategies effectively promoted the formation of high-quality DNA arrays, making it possible to arrange multiple probes in parallel with a high degree of uniformity. Moreover, we show that resultant arrays are compatible with standard hybridization protocols, which allowed for reliable discrimination of individual strands when exposed to a specific ssDNA target molecule.

KEYWORDS: DNA arrays • plastic substrates • microfluidic patterning

INTRODUCTION

DNA microarrays (also called DNA chips) (1−3) have become central to a variety of applications that include the mapping, monitoring, and sequencing of genes (2, 4), the discovery of novel drugs (5), and, more recently, the diagnostic of infectious diseases (6, 7). DNA microarrays typically comprise a set of presynthesized oligonucleotides immobilized on a solid support to be used for competitive hybridization with fluorescently labeled target genes. Thanks to the high specificity of interaction between complementary bases in the strands, a particular hybridization pattern is obtained for each array through fluorescence readout of the chip using a microarray scanner. Because the number of probes in an array determines the amount of information that can be extracted from a single experiment, high-density arrangement is a prerequisite for applications that involve precious and expensive samples or demand for a large number of probes to be screened in parallel.

There are two principal pathways to fabricate DNA chips. One method uses the principles of photolithography to synthesize in situ a desired sequence base by base (8). This process can yield arrays of high density (e.g., >2.5 × 10^5 probes per cm^2) but requires sophisticated instrumentation, which prevents its widespread use in standard microbiology laboratories. In addition, in situ synthesis is limited to relatively short oligonucleotides while high levels of redundancy are necessary because the yield of each synthesis step can vary. Another and generally more accessible way is microspotting, which involves the delivery of minute amounts of a DNA solution either through the robotic handling of metal pins (1, 9) or by use of drop-on-demand technologies (10, 11). The spot diameters that are obtained with current commercial arraying techniques are usually relatively large (e.g., between 500 and 80 μm, depending on the precision of the instrument, the experimental details of the spotting process, and the surface characteristics of the substrate). Although it has been demonstrated that spots ranging from the micrometer scale to below 100 nm can be realized when sufficiently miniaturized pins are employed (12, 13), much interest remains in the development of techniques that allow for routine access to spots of an intermediate size regime. For example, typical screening applications in medical diagnostics require only a limited number probes (e.g., less than 100), and spot diameters of 20−60 μm would facilitate accommodation of the corresponding arrays in appropriate lab-on-a-chip (LOC) devices (14, 15). The readout of spots of this size should still be straightforward using commercial microarray scanners that often support signal detection with a lateral resolution of ≥5 μm. However, spot uniformity remains a major problem associated with pin spotting,

* E-mail: matthias.geissler@cnrc-nrc.gc.ca.

Received for review April 28, 2009 and accepted June 17, 2009

DOI: 10.1021/am900285g

Published 2009 by the American Chemical Society

especially when performed on plastic substrates, demanding for stringent control over environmental conditions and processing parameters as well as surface modification procedures.

Traditionally, glass has been among the most favorable materials for DNA microarrays; it offers high mechanical stability and low intrinsic fluorescence background, and its surface can be modified with a variety of functional groups using silane chemistry (9). On the other hand, glass is relatively expensive and difficult to micromachine, motivating considerable research and development efforts toward plastic-based supports (16−22) for DNA arrays, especially when disposable, low-cost LOC platforms are the fabrication target. A number of hard thermoplastic materials including poly(methylmethacrylate) (PMMA), polycarbonate, or cyclic olefin copolymers seem promising to this end because these materials (i) are relatively inexpensive, (ii) provide robustness and durability at low specific weight, (iii) allow for large-scale replication using well-established techniques based on molding or embossing, and (iv) can be bonded (either permanently or reversibly) to other surfaces, which is key to the assembly and packaging of LOC devices. Furthermore, interfacial properties such as wetting, surface charge, compatibility with biological species, or reactivity toward functional groups can be altered conveniently for many polymers to comply with the requirements of a particular application. The use of optical-grade materials with low intrinsic fluorescence background constitutes another prerequisite for on-chip fluorescence-based detection of DNA hybridization events (20, 23, 24).

Microfluidics is generally perceived as a means of manipulating minute amounts of liquid using channels (or capillaries) with micrometer dimensions (25−28). Features that make the use of microfluidic systems advantageous are (i) low sample consumption, (ii) accurate registration and positioning, (iii) high parallelism, and (iv) good control over reaction conditions, among others. Flow in microchannels is typically characterized by low Reynolds numbers, with molecular diffusion being the dominant driving force in supplying reagents under the conditions of laminar flow. Convection can be achieved through implementation of bas-relief structures (29), split-and-recombine systems (30, 31), or multivortex segments (32). It is equally possible to employ several active methods such as magnetic stirring (33) or acoustic actuation (34). With the advent of soft lithography (35, 36), elastomer-based microcapillary systems (μCSs) became accessible to a broader scientific community, thus effectively promoting their use in surface processing and patterning. Elastomers are advantageous to a number of fluidic applications because these materials (i) conform to smooth substrates, (ii) provide a watertight seal to the surface, and (iii) can be removed from the substrate upon processing, often without leaving notable residues on the surface. The concept of fluidic patterning has been shown for a variety of materials; most notably, biological species such as DNA (16, 37), proteins (38−40), and cells (41, 42) immobilized silicon, glass, and plastic supports. At present, most fluidic-based arrays comprise a set of simple and continuous lines arranged in a parallel fashion, although the formation of discontinuous features using multilevel networks has also been demonstrated (42, 43). In addition to patterning, fluidic devices have come into focus as a means of performing amplification (44) or hybridization reactions (45−47) with oligonucleotides in a time- and cost-effective manner.

In this paper, we use microfluidics as means of fabricating DNA microarrays on hard thermoplastic substrates with excellent control over the size, density, and registration of spots. The μCS described herein comprises a two-dimensional (2D) network of microchannels, which are straightforward to fabricate by hot embossing using a melt-processable (thermoplastic) elastomer (48). The material is capable of sealing a surface reversibly upon contact, and the embedded microchannels can be filled by capillary action, that is, the autonomous movement of liquid in small channels based on hydrodynamic forces (43). Immobilization of DNA molecules is achieved through activation of the plastic surface with *N*-hydroxysuccinimide (NHS) and 1-ethyl-3-[3-(dimethylamino)propyl]carbodiimide hydrochloride (EDC) and subsequent passive incubation, although the design of the μCS would also allow for the connection of external pumping systems to induce continuous flow or recirculation of the probe liquid. Herein, we focus on the parameters affecting DNA attachment and investigate the conditions for obtaining high-quality microarrays of fluorescently labeled, amino-modified oligomers on substrates made from two commercially available polymers: PMMA and Zeonor 1060R. We believe that the work presented in this paper contributes to the development of integrated plastic LOC platforms for high-throughput diagnostics using DNA microarray technology.

RESULTS AND DISCUSSION

The μCSs that we used in this study were fabricated by hot embossing using sheets of Versaflex CL30, a styrenic block copolymer, in conjunction with a photolithographically prepared SU-8 master (49). Versaflex CL30 belongs to the class of thermoplastic elastomers (TPEs) and consists of hard polystyrene domains in a soft, rubbery matrix of poly(ethylene/butylene) (50). Inspection of the surface using atomic force microscopy (AFM) revealed a hexagonal arrangement of polystyrene domains, which are typically 10−30 nm in diameter (data not shown). The literature suggests that the size of these domains can range from micro- to nanometer length scales, being generally dependent on the processing conditions as well as on the molecular weight of the constituents (51, 52). Although few published examples exist on the use of TPEs for soft microfabrication, these polymers are currently finding increased attention in areas that traditionally rely on poly(dimethylsiloxane) (PDMS) (35, 36, 53−55) as the enabling material. For example, Trimbach and coworkers employed styrenic block copolymers for fabricating micropatterned elastomeric stamps for microcontact printing (μCP) (56). These authors further investigated the use of multiblock copolymers for producing stamps with a certain

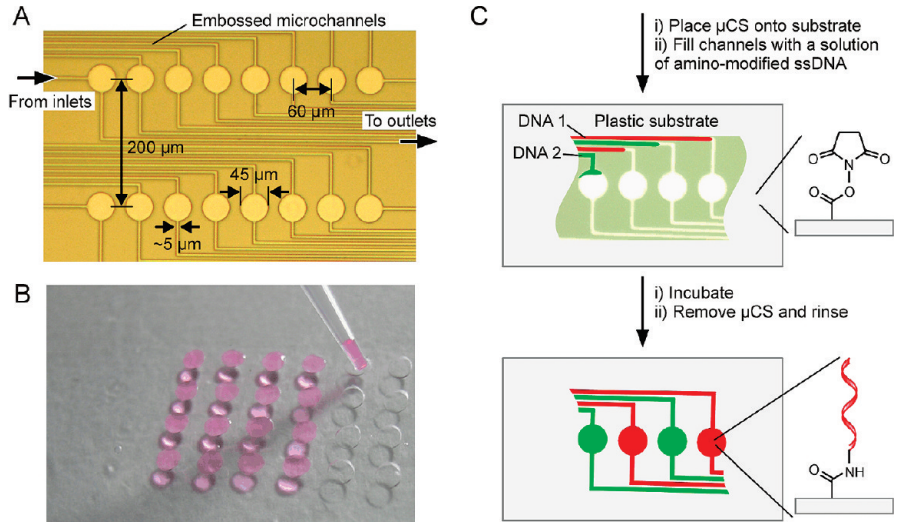

FIGURE 1. Microfluidic patterning of miniaturized DNA arrays on a plastic substrate. (A) Optical microscope image detailing the central area of a TPE-based μCS. (B) Photograph of the inlet part of a μCS on a Zeonor substrate during loading with a micropipet. The filled inlets (left-hand side of the array) contain each ~200 nL of solution of a Cy3-labeled oligonucleotide. Microfluidic supply channels connected to these inlets are too small to be visualized at this scale. The depth of the elastomer sheet (e.g., 150 μm) is apparent from unfilled inlets (right-hand side of the array). (C) Schematic illustration of the principles governing array formation. See the text for details.

degree of hydrophilicity (57). Huskens and co-workers demonstrated μCP using block copolymer stamps in conjunction with surface modification to transfer polar ink molecules onto a solid support (58). Moreover, Ugaz and co-workers employed tailored TPE gels for the fabrication of microfluidic networks (32, 59−61). Embossing of fluidic structures into CL30 was performed within the high-temperature regime of the elastomer, in which the polymer network softened, allowing the material to flow and adapt to the shape of the master pattern. Upon cooling, the material solidified, thereby preserving the shape of the imprinted features with high fidelity. The smallest feature size that we replicated in the context of this study was on the order of 5 μm, corresponding to the width of both ridges and trenches in the central part of the μCS (Figure 1A). Like for other elastomers such as PDMS, the mechanical stability of the microstructures was dependent on the aspect ratio (62, 63), allowing variation in the depth (d) of the microchannels to a limited extent. For example, the 5-μm-wide ridges could tolerate aspect ratios of up to 1.5 without notable deformation, yet these structures were prone to collapse when approaching an aspect ratio of 2.0 (64).

The central part of the μCS comprised a 2D array of circular cavities, each being 45 μm in diameter (Figure 1A). These features were arranged in rows with a periodicity of 60 μm. Arrays included up to 12 rows, providing a maximum number of 96 spots. Incoming and outgoing supply channels were ~5 μm in width but broadened to ~50 μm toward the periphery. The overall configuration of the μCS allows for producing DNA microarrays at relatively high density, while, in principle, being compatible with commercially available scanning technology for readout. We activated plastic substrates to achieve covalent attachment of amino-modified oligonucleotides using procedures that are described in more detail by Diaz-Quijada and co-workers (20). First, carboxylate groups were generated at the surface. For PMMA substrates, this was realized through base-catalyzed hydrolysis; Zeonor substrates were exposed to ozone gas. In a second step, carboxylic acid groups were converted into reactive esters through treatment with NHS and EDC (65). Microfluidic patterning was performed by placing the μCS channel side down onto an activated slide. Like other elastomers, CL30 can seal the surface reversibly, resulting in a full thermoplastic circuitry of enclosed microchannels. Each channel was filled from a macroscopic access point (inlet) into which we transferred ~200 nL of a DNA solution using a micropipet (Figure 1B). Displacement of the liquid within the fluidic systems occurred in a fully autonomous manner using capillary action. Pristine surfaces of Versaflex CL30 were largely hydrophobic, which necessitated hydrophilization of channels via oxygen plasma treatment to achieve capillary flow of aqueous DNA solutions, circumventing the need for adding any surfactants (66). Immobilization of DNA molecules takes place through displacement of the NHS ester and the formation of a stable amide bond, as depicted in Figure 1C. Finally, the array is recovered by peeling the μCS away from the surface. We validated the performance of the immobilization process using ssDNA in the form of relatively short oligonucleotides (probes p1−p5), which were modified with amino groups and labeled with either Cy3 (λ_{ex} = 550 nm; λ_{em} = 570 nm) or Cy5 (λ_{ex} = 650 nm; λ_{em} = 670 nm) fluorescent dye at the 3′ and 5′ positions of the strand, respectively (Table 1). The employment of fluorescently tagged oligonucleotides allowed for rapid and sensitive analysis of the resultant arrays using fluorescence microscopy.

Figure 2 illustrates the evolution of the fluorescence intensity (I) as a function of the incubation time and temperature for a 32 μM solution of p1 used in conjunction with a PMMA substrate. As shown by the images in Figure 2A, the incubation time was central to achieving DNA attachment at the plastic surface. While incubation for 1 h at 40 °C yielded only a faint fluorescence signal, a period of at least 6 h was required to reveal the array in a faithful

Table 1. Sequences and Modifications of Oligonucleotides Used in This Study

code	sequence	5′ end	3′ end
p1	CGGGCAGCATCAAGC	Cy3	$-(CH_2)_6NH_2$
p2	TTTTTTTTTT	Cy3	$-(CH_2)_6NH_2$
p3	TTTTTTTTTTTTTT	Cy5	$-(CH_2)_6NH_2$
p4	CGGGCAGACTCAAGC	Cy3	$-(CH_2)_6NH_2$
p5	TTTTTTTTTTTTTT	Cy3	$-(CH_2)_6NH_2$
t1	GCTTGATGCTGCCCG	none	Cy5

manner. When immobilization was allowed to proceed for longer durations (e.g., 48 h), the spots contrasted well with the bare plastic surface. In this example, the fluorescence intensity of the spots was about 15 times higher than that of the pristine PMMA substrate. Variation in the diameter of the spots was marginal (<5%) because the dimensions of the printed DNA features were defined by the design of the μCS and did not depend on the immobilization conditions or the wetting properties of the substrate. Edge definition of the spots was usually excellent: transition zones between modified and nonmodified regions were short (e.g., <5 μm) irrespective of the temperature and incubation time, suggesting that diffusion of DNA molecules along the surface into unexposed areas was limited for any of these conditions. This finding accounts for efficient sealing of the plastic surface by the elastomeric μCS (67). The images further

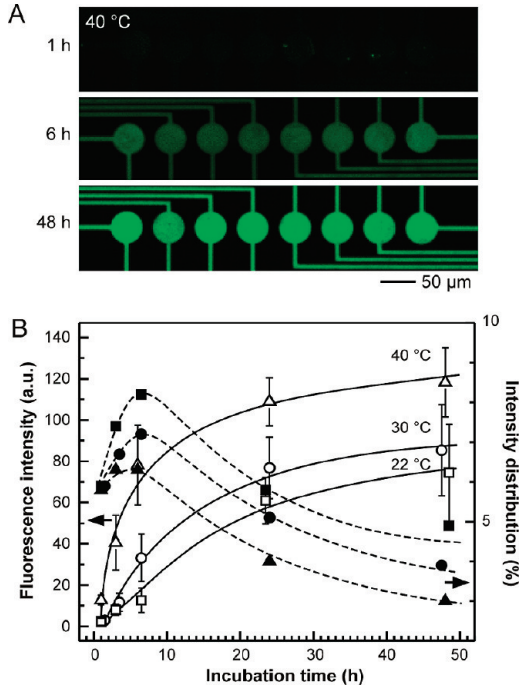

FIGURE 2. Kinetics of DNA adsorption on NHS-activated PMMA substrates as determined by fluorescence microscopy. (A) Fluorescence microscopic images of rows comprising 1 × 8 spots obtained from incubation with p1 at 40 °C for 1, 6, and 48 h. (B) Plots of the fluorescence intensity (open symbols, background-corrected) and the intensity distribution (filled symbols) as a function of the incubation time. Here, a DNA solution was incubated in a humidity chamber at 22, 30, and 40 °C (squares, circles, and triangles, respectively) for durations of between 1 and 48.5 h. The data were established by using a 32 μM solution of p1 in PBS and a μCS with d = 4.2 μm and $l \sim$ 20 mm. Lines in the graph serve as a guide to the eyes.

reveal that the fluorescence intensity was uniform among the spots in each array [e.g., with a coefficient of variation (CV) < 10%], which, however, was conditional to microfluidic supply channels being comparable in length (l) (see below).

It is apparent from Figure 2B that the immobilization process was sensitive to the temperature. Despite the fact that the density of immobilized probes increased when the temperature was raised from 22 to 30 and 40 °C, saturation of the surface was not achieved, indicating that the overall adsorption process was relatively slow under these experimental conditions. We think that hydrolysis did not reduce notably the overall yield of the immobilization process because the NHS ester on the plastic surface remained active for extended periods of time. This result was confirmed by control experiments in which we stored activated slides in a solution of PBS for up to 5 h before they were exposed to a solution of oligonucleotides (data not shown). When NHS ester groups were completely absent from the surface, DNA molecules adsorbed nonspecifically and were washed off the substrate in subsequent rinsing steps (data not shown). Distribution of the probes in the spotted areas was generally uniform, as can be concluded from the fact that variations in the fluorescence intensity were well below 10%. A slight increase in the intensity distribution was observed for shorter periods of incubation, however, corresponding to the formation of incomplete, low-density deposits during the initial phase of the immobilization process. After a maximum at ~10 h was passed, the uniformity of the deposits increased with the time of incubation for each of the inspected temperatures, although the best results were obtained when incubation was done at 40 °C.

Figure 3A illustrates the trends in the fluorescence intensity when we progressively reduced the concentration of p2 from 32 to 0.25 μM using fluidic structures that are 7.2, 4.2, and 1.4 μm in depth, respectively. As can be expected, the DNA concentration directly affects the fluorescence intensities, which decreased for spots produced with any of the three μCSs. The channel depth was equally important, and spots produced with structures that are 7.2 μm deep displayed the highest intensities among the three. This finding is consistent with the fact that a larger amount of DNA molecules can be transported in these channels compared to their shallower counterparts. In addition, surface area-to-volume ratios increased by a factor of 1.3 and 2.7 when d was reduced from 7.2 to 4.2 and 1.4 μm, respectively, for which depletion of the solution along trajectories became more pronounced. Histograms of individual spots mostly showed a narrow range of intensities (e.g., <10%) when concentrations of between 32 and 4 μM were used, suggesting homogeneous coverage of the surface with DNA molecules (Figure 3B). Spots of comparable quality are generally difficult to produce using conventional microspotting, where uncontrolled dewetting and drying of the solution often cause a notable variation in both the diameter and intensity of the resultant spots (68). We were not able to obtain any useful arrays for concentrations below 1 μM, for which the

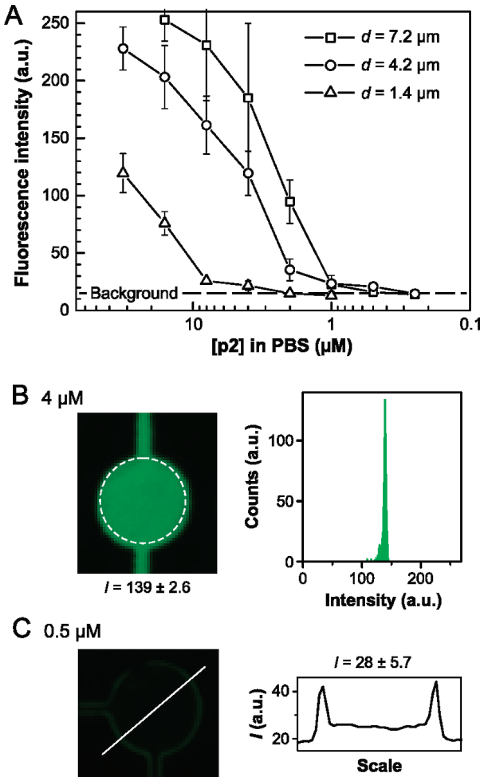

FIGURE 3. Probing the limits in the DNA concentration for microfluidic patterning. (A) Plot of a measured fluorescence signal as a function of the p2 concentration. The data were established using μCSs that were 7.2, 4.2, and 1.4 μm in depth (squares, circles, and triangles, respectively) in conjunction with an NHS-activated PMMA substrate. Incubation was done at 22 °C for ~16 h. (B and C) Fluorescence microscopic images of randomly selected spots that were obtained from 4 and 0.5 μM solutions of p2 in PBS. Distribution of DNA within these spots is illustrated by the respective histogram and cross-sectional view. In both cases, fluidic supply channels were ~10 mm long and 4.2 μm deep.

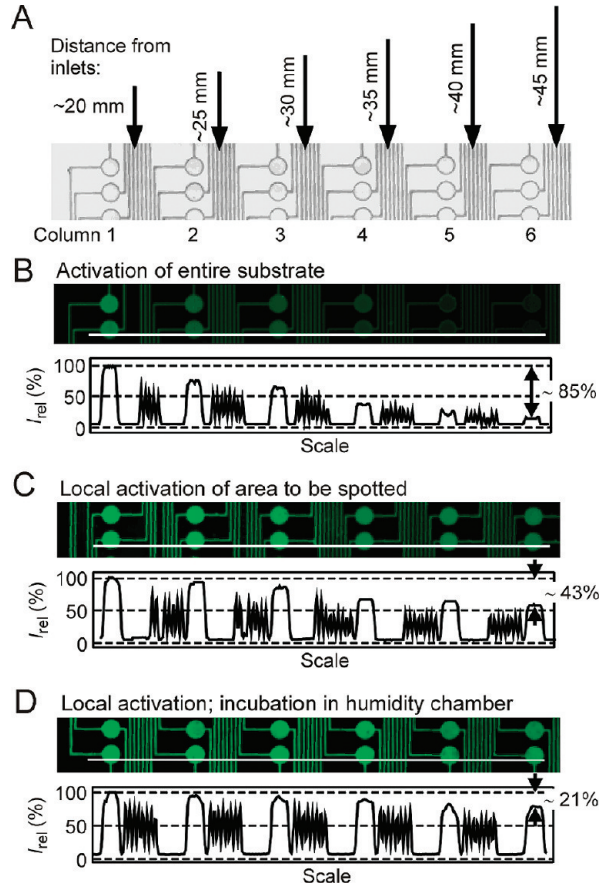

FIGURE 4. Effect of the channel length on the fluorescence intensity of the DNA spots on PMMA. (A) Design of a μCS comprising six columns of spots supplied by microchannels that are 20−45 mm long, respectively. Each set of channels is connected to one macroscopic inlet. Outgoing channels were 15 mm long. (B−D) Fluorescence microscopic images and corresponding intensity profiles detailing sections of 6 × 2 spots obtained from immobilization of p1 with PMMA at room temperature for 16 h. (B) Considerable decrease in the measured intensity with the channel length due to the unproductive loss of DNA molecules during transport when the entire surface of the substrate was activated with NHS and incubation was performed at ambient conditions. (C) Local activation of the substrate at the target area that notably reduced the loss of DNA molecules and improved the array uniformity to some extent for similar conditions of incubation. (D) Differences in the intensity of the spots that were marginal when a locally activated substrate and a humidity-controlled incubation chamber were used.

intensity values were approaching that of background fluorescence, even when used in conjunction with a μCS having a channel depth of 7.2 μm. We frequently observed that the fluorescence signal was confined to the edges of the fluidic structures (Figure 3C), especially when we allowed solutions with a lower DNA concentration to dry inside the channel system.

Depletion was, in addition to the handling of solutions with a low concentration of oligonucleotides, a limiting factor to the realization of uniform arrays when microfluidic supply channels showed notable differences in I. We demonstrated this effect by using a μCS providing an incremental increase in I over six columns of spots (Figure 4A). When a solution of p1 was incubated at ambient conditions, the resultant arrays displayed striking differences in I recorded for each column (Figure 4B). The resultant intensity decreased linearly from column 1 to 6 by ~85%, corresponding to an overall loss in the intensity of 3.4% mm^{-1}. With respect to the conditions of sample preparation, depletion was not the only origin of this relatively pronounced decay but rather was accompanied by irregular evaporation of the solvent during incubation. We were able to reduce the effect of depletion by confining treatment of the plastic surface with EDC/NHS instead of activating the entire surface of the plastic substrate. This was realized by spreading ~5 μL of the EDC/NHS solution over the central area of the plastic surface using a glass piece of ~1 cm^2 in size. With a substantial portion of the reactive area being eliminated along the pathway, selective activation not only led to increased values of I but also helped to reduce the gap in the intensity between columns relative to each other. For example, when NHS ester groups were present only at the last ~7 mm before the projected position of the array, the average intensities of the spots in column 6 were ~43% in comparison to their counterparts in column 1 (Figure 4C), suggesting a reduction in the fluorescence signal of 2.3% mm^{-1}. Although we did not elucidate the interaction of oligonucleotides and CL30, it was possible to reduce nonspecific adsorption to some extent by adding trace amounts of a surfactant such as sodium dodecylsulfate (SDS) to the

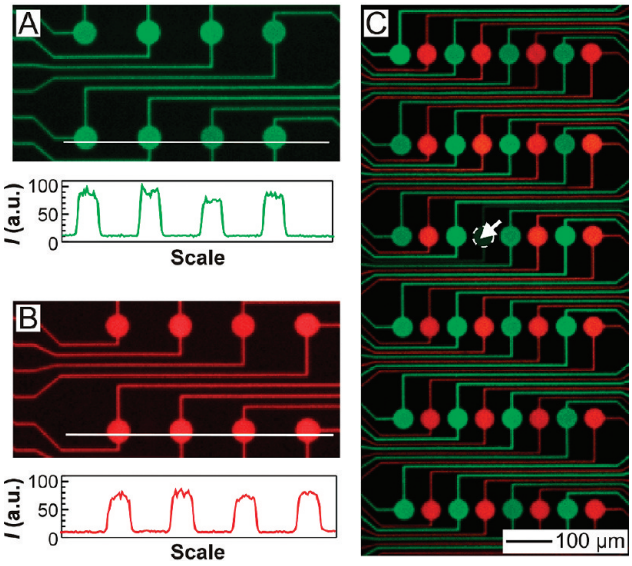

FIGURE 5. Parallel patterning of multiple probes. (A and B) Fluorescence micrographs and corresponding intensity profiles of a binary array comprising p1 and p3 as imaged in the Cy3 (green) and Cy5 (red) channels, respectively. Probes were immobilized on a Zeonor substrate using the same μCS. (C) Array of 6 $\times$ 8 spots obtained by a recombination of the images acquired in the Cy3 and Cy5 channels. The arrow marks the only spot in this array that was cross-contaminated.

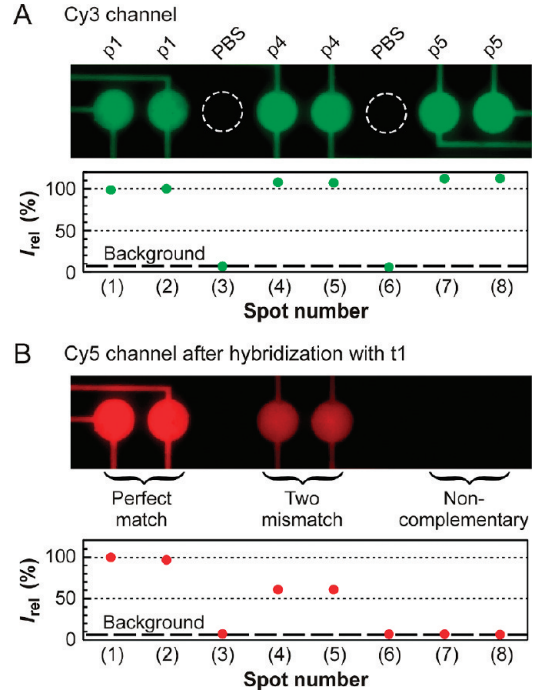

FIGURE 6. Hybridization assay comprising three DNA probes on PMMA and one target oligonucleotide. (A) Fluorescence microscopic image and the corresponding intensity profile of an array that was obtained from incubation with p1, p4, and p5, each having a concentration of 32 μM in PBS. The intensities were normalized by defining spot (2) as 100%. (B) Hybridization pattern (Cy5 emission) of the same array after passive incubation with t1. The plot shows the respective fluorescence intensities normalized with respect to spot (1).

DNA solution before incubation. However, the use of surfactants generally diminished the uniformity of the resultant spots, and we therefore did not pursue this approach any further.

Evaporation of the solvent affects the overall immobilization process by inducing convection and local changes in the concentration. Ultimately, the reaction comes to a halt once the channel has dried out. We suppressed evaporation by storing samples in a water-saturated atmosphere during incubation. When this was combined with the selective activation of the substrate, we were able to reduce variation in the fluorescence intensity to at least 21%, as shown in Figure 4D. Here, decay in the signal intensity corresponds to 0.84% mm^{-1}, which was primarily due to nonspecific adsorption of DNA molecules along trajectories. Increasing the temperature to 40 °C during incubation mainly resulted in higher signals for the entire array irrespective of the particular length of the supply channels. Even though we did not achieve perfect equilibration of the intensity values, the results obtained in the course of these experiments proved indispensible in successfully immobilizing DNA molecules throughout a larger number of spots while making it possible to maintain some flexibility in the design of μCSs.

Figure 5 depicts the result of incubating two probes (e.g., p1 and p3) in parallel that were arranged in an alternating manner. We observed fluorescence emission of the respective dyes only in the exposed regions of the plastic surface (Figure 5A,B), indicating that probes remained effectively isolated from each other. The number of sites showing signs of cross-contamination was ~5% on average, making it possible to achieve nearly perfect arrays (e.g., 48 spots) on a routine basis, for which an example is shown in Figure 5C. Proper surfaces of both the substrate and μCS were a prerequisite for obtaining arrays with no or minimal cross-contamination, making it necessary to assemble the two components in a filtered (e.g., clean-room) environment. Figure 5C further confirms that the periodicity of the spots in both x and y directions varied marginally, accounting for excellent registration of the spots with respect to one another. However, we determined that the overall area of the printed array was reduced by ~2% in size compared to that of the original SU-8 master pattern. This finding was mainly due to shrinkage of the elastomer sheet upon release from the mold, an effect that may be reduced by optimizing the processing parameters, such as the temperature, pressure, and embossing time.

Figure 6 summarizes the outcome of a hybridization experiment that involved three different oligonucleotide probes that were immobilized on a PMMA substrate. We selected p1, p4, and p5, all of which are amino-modified 15-mers labeled with Cy3 (Table 1). The sequence of these molecules differed, however, because p1 and p4 showed mismatches for two consecutive bases (CA versus AC, respectively), while p5 was exclusively composed of T. Figure 6A displays a test array comprising sets of two neighboring spots for each probe, which are separated by PBS serving as a negative control. Cy3 fluorescence intensities were almost equal for spots of the same probe (CV < 2%) but varied slightly between the three different sets (CV < 10%). Negative controls were indistinguishable from the bare regions of the PMMA substrate. We did not detect any

fluorescence intensity above the background level when we screened the array for Cy5 emission (data not shown). Probes were subjected to hybridization with t1, a Cy5-labeled oligonucleotide that had a sequence complementary to p1 (Table 1). As can be predicted, the fluorescence intensity varied when the array was subsequently imaged in the Cy5 channel. While hybridized spots corresponding to p1 showed the highest intensity, spots of p4 were both revealed faithfully but emitted a significantly less fluorescence signal (Figure 6B). We did not detect any notable fluorescence for spots of p5 as well as for the PBS control. The initial uniformity among the probes was largely preserved in the hybridization pattern (CV $\sim$ 3%), which allowed the probes to be discriminated in a reliable manner. The difference in Cy5 fluorescence emission between t1 hybridized to p1 and p4 was $\sim$40%, which accounts for a significant reduction in affinity between these chains as induced by a mismatch of two neighboring base pairs.

CONCLUSION

The patterning of DNA arrays benefits from the use of μCSs in a number of ways, which include (i) good control over immobilization conditions, (ii) limited dependency on the wetting properties of a particular substrate, and (iii) excellent alignment and registration capabilities. We believe that the demonstrations presented in this paper are encouraging and offer the potential for further development. While we exclusively focused on PMMA and Zeonor substrates, the process described herein should be applicable to a broad range of other materials without the need of drastically altering experimental protocols. It is also possible to extend the current design to arrays supporting a larger number of spots. It is likely, however, that the footprint of the μCS increases as a result, which may be a constraint with respect to the shape and size of the substrates to be used. Moreover, the current design may encounter limitations in the array density that may be achievable. Here, the development of multilevel systems comprising open through-hole membranes may be helpful in overcoming this constraint to some extent. Although we have shown that printed DNA microarrays are fully compatible with standard hybridization protocols, limits in detection, especially in conjunction with nonlabeled oligonucleotide probes, remain to be addressed. The volume of the DNA solution used for producing a single spot in the array was relatively high (e.g., $\sim$200 nL), mainly to counterbalance the effect of evaporation during transfer in the absence of proper equipment and the lack of control over environmental conditions. Improvement of the experimental settings should make it possible to overcome this obstacle, allowing volumes to be reduced significantly for the approach to become economically favorable. For example, recent experiments indicated that it is possible to use slotted metal pins instead of a micropipet, which can be arranged as a set that enable the liquid to be transferred in a parallel rather than a sequential fashion (48). Beyond its application in the area of DNA chips, similar or related systems are likely to find attention in a number of other areas, including protein crystallization, drug screening, or cell communication studies. As demonstrated in this article, CL30 is a suitable material for fabricating 2D μCSs because it provides a watertight seal of plastic surfaces, making it possible to confine a solution of reagents with high spatial control. Although the use of an inexpensive, melt-processable elastomer is an incentive for rapid prototyping of disposable microfluidic systems, it remains to be explored whether CL30 can live up to the challenges that fluidic technologies are facing in terms of cost-efficiency, performance, and integration. Clearly, many of the properties relevant in this context, such as thermal or mechanical behavior, permeability to solvents, or the effect of ingredients present in the polymer, were not within the scope of this study. Some of the main characteristics of this material are addressed in a separate publication (48), while others await further investigation. In addition, the development of methods to functionalize the surface and tailor interfacial properties in a chemically well-defined manner will be necessary to promote widespread acceptance of CL30 in soft microfabrication.

EXPERIMENTAL SECTION

Fabrication of μCSs. Fluidic structures were imprinted into Versaflex CL30 (GLS Corp., McHenry, IL) using a mold that was prepared by photolithography using SU-8 (GM1040; Gersteltec, Pully, Switzerland) on a 4 or 6 in. silicon wafer (Silicon Quest International, Inc., Santa Clara, CA). For fabrication of a mold, the wafer was first baked on a hot plate at 160 °C for 15 min; a SU-8 resist was applied through spin coating, which was followed by a prebake at 65 and 95 °C for 5 and 15 min, respectively, using a temperature ramp of 2 °C min^{-1}. The resist was exposed to UV light with a wavelength of 365 nm (Hg i-line) at 280 μJ cm^{-2} through a quartz/Cr mask (HTA Photomask, San Jose, CA) using an EVG 6200 mask aligner (EV Group, Schärding, Austria). A postexposure bake was done using the same conditions as those for the prebake. The resist features were developed in propylene glycol monomethyl ether acetate (Sigma-Aldrich Corp., St. Louis, MO) for 2 min; the wafer was rinsed with isopropyl alcohol (Anachemia, Montréal, Quebec, Canada) and dried with a stream of nitrogen gas. The resultant resist pattern was hard-baked at 130 °C for 2 h. Finally, the master was coated with a thin, antiadhesive layer formed from *1H,1H,2H,2H*-perfluorooctyltrichlorosilane (Aldrich) using deposition from the vapor phase under reduced pressure. CL30 was received in the form of pellets; the material was extruded at 165 °C to yield a film that was $\sim$150 μm in thickness. The film was cut into pieces of the appropriate size, which were imprinted with the master using an EVG 520 embossing tool (EV Group) operated at 170 °C, an applied force of 2×10^3 N over the entire area of the wafer, and a pressure of 1×10^{-3} mbar. Upon cooling to room temperature, the micropatterned elastomer piece was peeled off the master and cut to its final size. Inlets were typically punched through the material; occasionally channels were opened by cutting off their periphery. Prior to use, fluidic devices were exposed to oxygen plasma (Plasmalab80Plus from Oxford Instruments, Bristol, U.K.) for 4 min at 100 W, a flux of 20 sccm, and a pressure of 50 mTorr. All fabrication steps were carried out in a clean-room environment (class 1000).

Preparation of Substrates. Plastic substrates were prepared from either PMMA (Plexiglas VS UVT, Altuglas International, Philadelphia, PA) or Zeonor 1060R (Zeon Chemicals, Louisville, KY). PMMA slides of standard size (25×75 mm^2 in area; 1 mm in thickness) were fabricated by injection molding using a Boy

30A injection tool (Dr. Boy GmbH, Neustadt-Fernthal, Germany) operated at a temperature of 220−240 °C, an injection speed of 30 mm s^{-1}, and a pressure of 132 bar. The mold (stainless steel, custom-fabricated) was cooled for 15 s before the slide was released. Zeonor disks (6 in. in diameter) were molded using an Engel 150 injection apparatus (Engel, Schwertberg, Austria) operated at temperatures between 127 and 134 °C, an injection speed of 45−103 mm s^{-1}, and a pressure of 25 bar. Plastic substrates were incubated with methanol (Fisher Scientific, Ottawa, Ontario, Canada) for ∼20 min before surface modification. PMMA slides were incubated with a saturated aqueous solution of sodium hydroxide (Sigma-Aldrich) for ∼2 h, including 1 h of ultrasonication. Each slide was thoroughly rinsed with deionized (DI) water (18.2 MΩ cm, Millipore, Billerica, MA) and dried with a stream of nitrogen gas. Zeonor substrates were subjected to ozone treatment for ∼20 min. The setup consisted of an Ozo 2vtt ozone generator (OzoMax, Inc., Shefford, Quebec, Canada) connected to a home-built glass chamber (∼20 cm in diameter); samples were placed on a rotary holder stage inside the chamber to ensure uniform treatment. Substrates were then incubated with a freshly prepared solution of 2 mg (17 μmol) of NHS (Sigma-Aldrich) and 8 mg (42 μmol) of EDC (Sigma-Aldrich) in 100 μL of phosphate-buffered saline (PBS, pH 7.4, Sigma-Aldrich). We applied ∼3 μL of solution per cm^2 of surface area; the solution was spread over the substrate via contact with a glass microscope slide, and the sample was stored in a glass or polystyrene Petri dish (Sigma-Aldrich) at room temperature for ∼90 min. Upon removal of the cover slide, the sample was rinsed with DI water and dried with a stream of nitrogen gas.

Formation of DNA Arrays. Oligonucleotides were purchased from Integrated DNA Technologies, Inc. (Coralville, IA), and used without further purification. Solutions of PBS with concentrations ranging from 32 to 0.25 μM were used for patterning experiments. The TPE-based μCS was placed the channel side down onto the surface of a freshly activated substrate; contact between the two formed instantaneously and typically propagated across the entire surface without the need for applying any additional force. Charging was done by placing ∼200 nL of a DNA solution at each channel inlet using a micropipet. During incubation, samples were kept in a Petri dish or glass container of the appropriate size covered with aluminum foil in order to prevent photoinduced bleaching of fluorescence dyes. Incubation was done at 22, 30, or 40 °C for various durations (see the text for details). The humidity chamber used in this study comprised a water-containing beaker, which was sealed with Parafilm against evaporation. Upon incubation, the μCS was removed from the substrate while being immersed in a 0.1% solution of SDS (Sigma-Aldrich) in PBS. Upon removal from the solution, the substrate was rinsed with DI water to wash nonimmobilized DNA molecules off the surface, followed by drying with a stream of nitrogen gas. Each μCS was used once to prevent interference with previous experiments.

Hybridization. Samples were subjected to hybridization without any prior deactivation step. Arrays were incubated with 25 μL of a 10 μM solution of t1 in PBS; the solution was spread over the surface through contact with a microscope glass cover slide, and the sample was stored at room temperature in a light-protective container for 3 h. Upon removal of the coverslip, the substrate was carefully rinsed first with a 0.1% solution of SDS in PBS and then with water and finally dried with a stream of nitrogen gas.

Instrumentation. Angles of contact were measured with a contact-angle goniometer (model 200-F1) from Ramé-Hart Instrument Co. (Netcong, NJ) using DI water as the probe liquid. Images of advancing and receding drops were recorded with a CCD camera and analyzed using *DROPimage Standard* software. AFM measurements were done using a multimode Nanoscope IV atomic force microscope (Veeco Metrology Group, Santa Barbara, CA), operated at ambient conditions and in contact mode using silicon nitride cantilevers (NP-S20, Veeco) with a spring constant of 0.58 N m^{-1}. For each sample, an area of 3 × 3 μm^2 was imaged at a rate of ∼1.0 Hz and a pixel resolution of 512 × 512. Fluorescence imaging of DNA arrays was performed using an Eclipse TE2000-U inverted fluorescence microscope from Nikon (Melville, NY) equipped with an EM-CCD camera from Hamamatsu (Bridgewater, NJ). For each series of samples, identical settings of data acquisition were used to allow for comparison of the detected fluorescence signals. It should be noted, however, that the conditions of imaging varied between different sets of samples. Fluorescence intensities were quantified using *ImageJ*, a Java-based processing and analysis software (downloaded at http://rsb.info.nih.gov/ij/download.html). Optical micrographs were taken using a Nikon Eclipse L150 optical microscope equipped with a QICAM fast digital camera from QImaging Corp. (Burnaby, British Columbia, Canada).

Acknowledgment. This work was supported, in part, by Genome Canada and Génome Québec. We thank Dr. Régis Peytavi (Université Laval) and Dr. André Nantel (BRI/CNRC) for useful discussion and our colleagues Kien-Mun Lau, Jimmy Chrétien, Michel Carmel, Yves Simard, Hélène Roberge, François Normandin, and Sylvie Bérardi (BRI/CNRC) for technical assistance. We are grateful to Prof. Michel G. Bergeron (Université Laval) and Dr. Michel M. Dumoulin (IMI/CNRC) for their support.

Note Added after ASAP Publication. Due to a production error, this paper was published ASAP on July 10, 2009, with a number of minor text and reference errors. The correct version was posted on July 14, 2009.

REFERENCES AND NOTES

(1) *Microarray Biochip Technology*; Schena, M., Ed.; Eaton Publishing: Natick, MA, 2000.
(2) Review: Lockhart, D. J.; Winzeler, E. A. *Nature* **2000**, *405*, 827–836.
(3) Review: Heller, M. J. *Annu. Rev. Biomed. Eng.* **2002**, *4*, 129–153.
(4) Higgins, J. P. T.; Shinghal, R.; Gill, H.; Reese, J. H.; Terris, M.; Cohen, R. J.; Fero, M.; Pollack, J. R.; van de Rijn, M.; Brooks, J. D. *Am. J. Pathol.* **2003**, *162*, 925–932.
(5) Review: Debouck, C.; Goodfellow, P. N. *Nat. Genet.* **1999**, *21*, 48–50.
(6) Peytavi, R.; Raymond, F. R.; Gagné, D.; Picard, F. J.; Jia, G.; Zoval, J.; Madou, M.; Boissinot, K.; Boissinot, M.; Bissonnette, L.; Ouellette, M.; Bergeron, M. G. *Clin. Chem.* **2005**, *51*, 1836–1844.
(7) Dawson, E. D.; Moore, C. L.; Smagala, J. A.; Dankbar, D. M.; Mehlmann, M.; Townsend, M. B.; Smith, C. B.; Cox, N. J.; Kuchta, R. D.; Rowlen, K. L. *Anal. Chem.* **2006**, *78*, 7610–7615.
(8) Lipschutz, R. J.; Fodor, S. P. A.; Gingeras, T. R.; Lockhart, D. J. *Nat. Genet.* **1999**, *21*, 20–24.
(9) Review: Pirrung, M. C. *Angew. Chem., Int. Ed.* **2002**, *41*, 1276–1289.
(10) Okamoto, T.; Suzuki, T.; Yamamoto, N. *Nat. Biotechnol.* **2000**, *18*, 438–441.
(11) Gutmann, O.; Kuehlewein, R.; Reinbold, S.; Niekrawietz, R.; Steinert, C. P.; de Heij, B.; Zengerle, R.; Daub, M. *Biomed. Microdevices* **2004**, *6*, 131–137.
(12) Xu, J.; Lynch, M.; Huff, J. L.; Mosher, C.; Vengasandra, S.; Ding, G.; Henderson, E. *Biomed. Microdevices* **2004**, *6*, 117–123.
(13) Demers, L. M.; Ginger, D. S.; Park, S.-J.; Li, Z.; Chung, S.-W.; Mirkin, C. A. *Science* **2002**, *296*, 1836–1838.
(14) *Lab on a Chip*, a series of insight review articles in *Nature* **2006**, *442*, 367−418.
(15) Review: Madou, M.; Zoval, J.; Jia, G.; Kido, H.; Kim, J.; Kim, N. *Annu. Rev. Biomed. Eng.* **2006**, *8*, 601–628.
(16) Li, Y.; Wang, Z.; Ou, L. M. L.; Yu, H.-Z. *Anal. Chem.* **2007**, *79*, 426–433.

(17) Fixe, F.; Dufva, M.; Tellemann, P.; Christensen, C. B. V. *Nucleic Acids Res.* **2004**, *32*, e9/1−e9/8.
(18) Bi, H.; Meng, S.; Li, Y.; Guo, K.; Chen, Y.; Kong, J.; Yang, P.; Zhong, W.; Liu, B. *Lab Chip* **2006**, *6*, 769–775.
(19) Lin, R.; Burns, M. A. *J. Micromech. Microeng.* **2005**, *15*, 2156–2162.
(20) Diaz-Quijada, G. A.; Peytavi, R.; Nantel, A.; Roy, E.; Bergeron, M. G.; Dumoulin, M. M.; Veres, T. *Lab Chip* **2007**, *7*, 856–862.
(21) Liu, Y.; Rauch, C. B. *Anal. Biochem.* **2003**, *317*, 76–84.
(22) Situma, C.; Wang, Y.; Hupert, M.; Barany, F.; McCarley, R. L.; Soper, S. A. *Anal. Biochem.* **2005**, *340*, 123–135.
(23) Noerholm, M.; Bruus, H.; Jakobsen, M. H.; Telleman, P.; Ramsing, N. B. *Lab Chip* **2004**, *4*, 28–37.
(24) Hawkins, K. R.; Yager, P. *Lab Chip* **2003**, *3*, 248–252.
(25) Stone, H. A.; Stroock, A. D.; Ajdari, A. *Annu. Rev. Fluid Mech.* **2004**, *36*, 381–411.
(26) Materials for Micro- and Nanofluidics, a special issue of *MRS Bull.* **2006**, *31*, 87−124.
(27) Review: Squires, T. M.; Quake, S. R. *Rev. Mod. Phys.* **2005**, *77*, 977–1026.
(28) Review: Delamarche, E.; Juncker, D.; Schmid, H. *Adv. Mater.* **2005**, *17*, 2911–2933.
(29) Stroock, A. D.; Dertinger, S. K. W.; Ajdari, A.; Mezić, I.; Stone, H.; Whitesides, G. M. *Science* **2002**, *295*, 647–651.
(30) Dertinger, S. K. W.; Chiu, D. T.; Jeon, N. L.; Whitesides, G. M. *Anal. Chem.* **2001**, *73*, 1240–1246.
(31) Jeon, N. L.; Dertinger, S. K. W.; Chiu, D. T.; Choi, I. S.; Stroock, A. D.; Whitesides, G. M. *Langmuir* **2000**, *16*, 8311–8316.
(32) Sudarsan, A. P.; Ugaz, V. M. *Proc. Natl. Acad. Sci. U.S.A.* **2006**, *103*, 7228–7233.
(33) Lu, L.-H.; Ryu, K. S.; Liu, C. *J. Microelectromech. Syst.* **2002**, *11*, 462–469.
(34) Liu, R. H.; Yang, J.; Pindera, M. Z.; Athavale, M.; Grodzinski, P. *Lab Chip* **2002**, *2*, 151–157.
(35) Review: Xia, Y.; Whitesides, G. M. *Angew. Chem., Int. Ed.* **1998**, *37*, 551–575.
(36) Review: Michel, B.; Bernard, A.; Bietsch, A.; Delamarche, E.; Geissler, M.; Juncker, D.; Kind, H.; Renault, J.-P.; Rothuizen, H.; Schmid, H.; Schmidt-Winkel, P.; Stutz, R.; Wolf, H. *IBM J. Res. Dev.* **2001**, *45*, 697–719.
(37) Chen, H.; Wang, L.; Li, P. C. H. *Lab Chip* **2008**, *8*, 826–829.
(38) Delamarche, E.; Bernard, A.; Schmid, H.; Michel, B.; Biebuyck, H. A. *Science* **1997**, *276*, 779–781.
(39) Delamarche, E.; Bernard, A.; Schmid, H.; Bietsch, A.; Michel, B.; Biebuyck, H. *J. Am. Chem. Soc.* **1998**, *120*, 500–508.
(40) Bernard, A.; Michel, B.; Delamarche, E. *Anal. Chem.* **2001**, *73*, 8–12.
(41) Takayama, S.; McDonald, J. C.; Ostuni, E.; Liang, M. N.; Kenis, P. J. A.; Ismagilov, R. F.; Whitesides, G. M. *Proc. Natl. Acad. Sci. U.S.A.* **1999**, *96*, 5545–5548.
(42) Chiu, D. T.; Jeon, N. L.; Huang, S.; Kane, R. S.; Wargo, C. J.; Choi, I. S.; Ingber, D. E.; Whitesides, G. M. *Proc. Natl. Acad. Sci. U.S.A.* **2000**, *97*, 2408–2413.
(43) Juncker, D.; Schmid, H.; Drechsler, U.; Wolf, H.; Wolf, M.; Michel, B.; de Rooij, N.; Delamarche, E. *Anal. Chem.* **2002**, *74*, 6139–6144.
(44) Review: Zhang, C.; Xu, J.; Ma, W.; Zheng, W. *Biotechnol. Adv.* **2006**, *24*, 243–284.
(45) Lee, H. H.; Smoot, J.; McMurray, Z.; Stahl, D. A.; Yager, P. *Lab Chip* **2006**, *6*, 1163–1170.
(46) Benn, J. A.; Hu, J.; Hogan, B. J.; Fry, R. C.; Samson, L. D.; Thorsen, T. *Anal. Biochem.* **2006**, *348*, 284–293.
(47) Lee, H. J.; Goodrich, T. T.; Corn, R. M. *Anal. Chem.* **2001**, *73*, 5525–5531.
(48) Roy, E.; Geissler, M.; Galas, J.-C.; Diaz-Quijada, G. A.; Veres, T. *Lab Chip* **2009**, submitted for publication.
(49) Shaw, J. M.; Gelorme, J. D.; LaBianca, N. C.; Conley, W. E.; Holmes, S. J. *IBM J. Res. Dev.* **1997**, *41*, 81–94. The process conditions for obtaining high-quality patterns with this resist are relatively well established. In addition, SU-8 is stable over a wide range of temperatures and mechanically more robust than many other resist formulations, which enabled us to reuse the same master for several embossing cycles without notable degradation.
(50) *Handbook of Thermoplastic Elastomers*, 2nd ed.; Walker, B. M., Rader, C. P., Eds.; Van Nostrand Reinhold Co., Inc.: New York, 1988.
(51) Review: Fredrickson, G. H.; Bates, F. S. *Annu. Rev. Mater. Sci.* **1996**, *26*, 501–550.
(52) Motomatsu, M.; Mizutani, W.; Tokumoto, H. *Polymer* **1997**, *38*, 1779–1785.
(53) Review: Quake, S. R.; Scherer, A. *Science* **2002**, *290*, 1536–1540.
(54) Review: McDonald, J. C.; Whitesides, G. M. *Acc. Chem. Res.* **2002**, *35*, 491–499.
(55) Geissler, M.; Kind, H.; Schmidt-Winkel, P.; Michel, B.; Delamarche, E. *Langmuir* **2003**, *19*, 6283–6296.
(56) Trimbach, D.; Feldman, K.; Spencer, N. D.; Broer, D. J.; Bastiaansen, C. W. M. *Langmuir* **2003**, *19*, 10957–10961.
(57) Trimbach, D. C.; Al-Hussein, M.; de Jeu, W. H.; Decré, M.; Broer, D. J.; Bastiaansen, C. W. M. *Langmuir* **2004**, *20*, 4738–4742.
(58) Sadhu, V. B.; Perl, A.; Péter, M.; Rozkiewicz, D. I.; Engbers, G.; Ravoo, B. J.; Reinhoudt, D. N.; Huskens, J. *Langmuir* **2007**, *23*, 6850–6855.
(59) Sudarsan, A. P.; Ugaz, V. M. *Anal. Chem.* **2004**, *76*, 3229–3235.
(60) Sudarsan, A. P.; Wang, J.; Ugaz, V. M. *Anal. Chem.* **2005**, *77*, 5167–5173.
(61) Sudarsan, A. P.; Ugaz, V. M. *Lab Chip* **2006**, *6*, 74–82.
(62) Delamarche, E.; Schmid, H.; Michel, B.; Biebuyck, H. *Adv. Mater.* **1997**, *9*, 741–746.
(63) Bietsch, A.; Michel, B. *J. Appl. Phys.* **2000**, *88*, 4310–4318.
(64) Versaflex CL30 has a surface hardness of 30 (shore A), a tensile strength of 6619 kPa, and an elongation at break of 780% according to the specifications of the supplier. Accessed at http://www.glscorp.com.
(65) EDC/NHS coupling chemistry is frequently used for the immobilization of biochemical species containing amino functionalities. EDC reacts with carboxylic acid groups at the surface to form a reactive *O*-acylisourea intermediate, which is subsequently converted into an NHS ester species. The ester functionality provides higher stability than the reactive intermediate, allowing two-step coupling procedures with amine-modified DNA or proteins to be performed in a controlled fashion and without affecting carboxylic acid groups that may be present in these molecules. For example, see: Johnsson, B.; Löfås, S.; Lindquist, G. *Anal. Biochem.* **1991**, *198*, 268–277.
(66) Extruded pieces of CL30 that were used for device fabrication exhibited advancing (θ_{adv}) and receding (θ_{rec}) contact angles of $108 \pm 1°$ and $84 \pm 1°$, respectively. Exposure to oxygen plasma (e.g., 100 W and 20 sccm for 4 min) rendered the surface somewhat more hydrophilic. After rinsing any possible residues off the surface, we obtained θ_{adv} and θ_{rec} of $65 \pm 2°$ and $21 \pm 4°$, respectively, which were sufficient to promote autonomous movement of aqueous solution in the channels. The time required for filling the entire μCS is dependent on l and was typically on the order of 5−15 min. Oxidized surfaces of CL30 were sufficiently stable in air to ensure convenient handling, yet they largely recovered their hydrophobic character over the course of several days when stored at ambient conditions.
(67) AFM measurements of activated plastic surfaces revealed root-mean-square roughness values that were generally in the lower nanometer range for both PMMA and Zeonor substrates. The μCS conformed spontaneously to either of these surfaces without the need for applying any external pressure. Forces of adhesion between CL30 and Zeonor were generally superior to those of CL30 and PMMA (data not shown), indicating differences in the polymer−polymer interactions at the interface.
(68) Deegan, R. D.; Bakajin, O.; Dupont, T. F.; Huber, G.; Nagel, S. R.; Witten, T. A. *Nature* **1997**, *389*, 827–829.

AM900285G